

Structural simplicity as a restraint on the structure of amorphous silicon

Matthew J. Cliffe*, Albert P. Bartók, Rachel N. Kerber,
Clare P. Grey, Gábor Csányi, and Andrew L. Goodwin

June 5, 2017

Department of Chemistry, University of Cambridge,
Lensfield Road, Cambridge, CB2 1EW, U.K.

*To whom correspondence should be addressed; e-mail: mjc222@cam.ac.uk.

Contents

1 Full list of configurations	2
-------------------------------	---

List of Figures

1 Coordination number distributions	3
2 PDFs	4
3 Bond angle distributions	5
4 Dihedral angle distribution	6
5 Q_l coefficients	7
6 Ring statistics	8
7 RMSD on optimisation	9
8 Tightbinding EDoS	10
9 MBJ DFT EDoS	11
10 MBJ DFT EDoS around gap	12
11 Diffraction pattern comparison	15

List of Tables

1 Energies	13
2 Metrics of fits	14

1 Full list of configurations

All configurations are 512 atoms, in a 21.7 Å cubic box. All RMC refined configurations were refined for 128 million attempted moves.

Random A random configuration, with no other constraints.

Hard sphere A random configuration, generated with the constraint that no atom be placed within 2.2 Å of another.

RMC A random configuration refined against PDF data taken from a 4096 atom WWW configuration using RMC, with no other constraints.

RMC relax The RMC configuration optimised with DFT using the PBE functional until convergence.

INVERT A random configuration refined against PDF data taken from a 4096 atom WWW configuration using RMC, with the INVERT PDF variance restraint applied^{S1}.

INVERT relax The INVERT configuration optimised with DFT using the PBE functional until convergence.

SPH A random configuration refined against PDF data taken from a 4096 atom WWW configuration using RMC, with the INVERT PDF variance restraint, the spherical harmonic bond-orientational order parameter variance constraint, and the spherical harmonics local symmetry restraint applied^{S1, S2}.

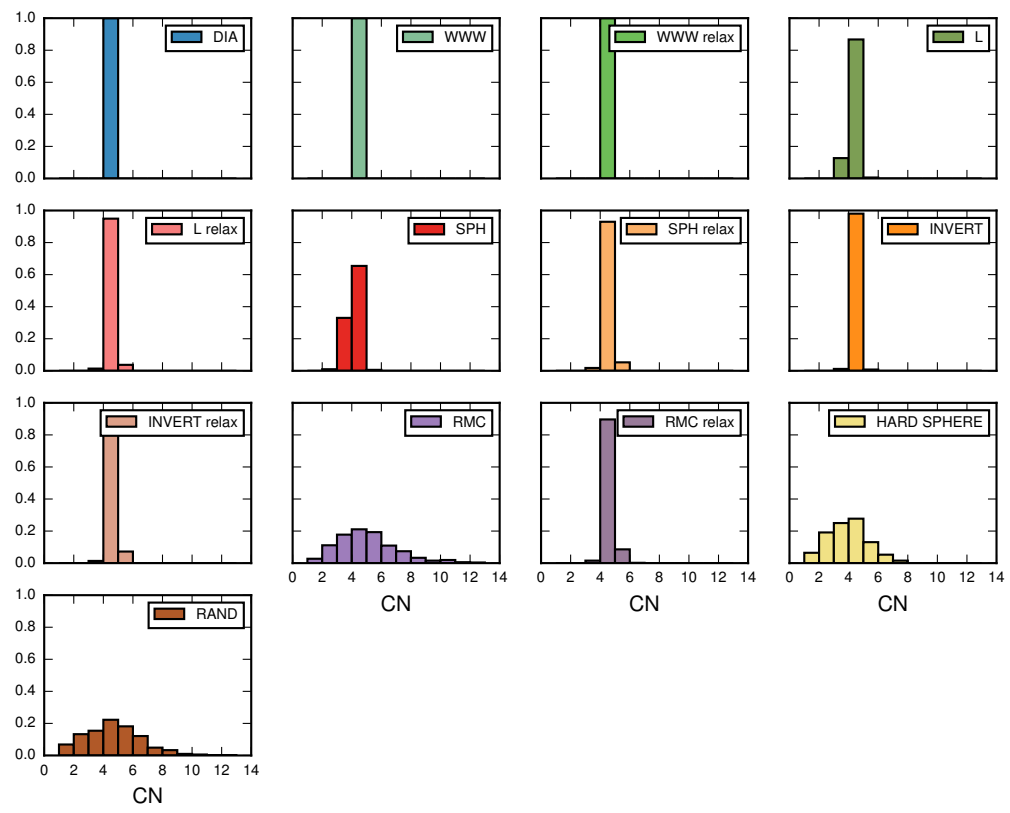
SPH relax The SPH configuration optimised with DFT using the PBE functional until convergence.

L A random configuration refined against PDF data taken from a 4096 atom WWW configuration using RMC, with the SOAP self-similarity restraint **L** also applied^{S3}.

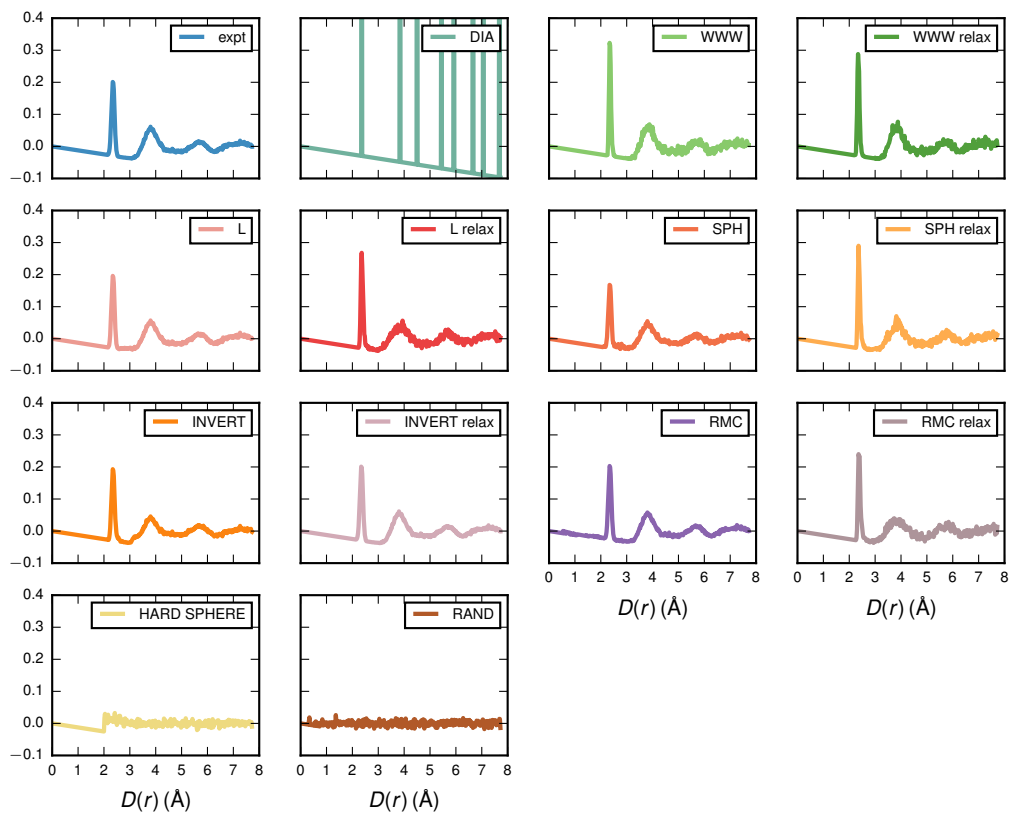
L relax **L** optimised with DFT using the PBE functional until convergence.

WWW A configuration generated using the WWW algorithm^{S4}.

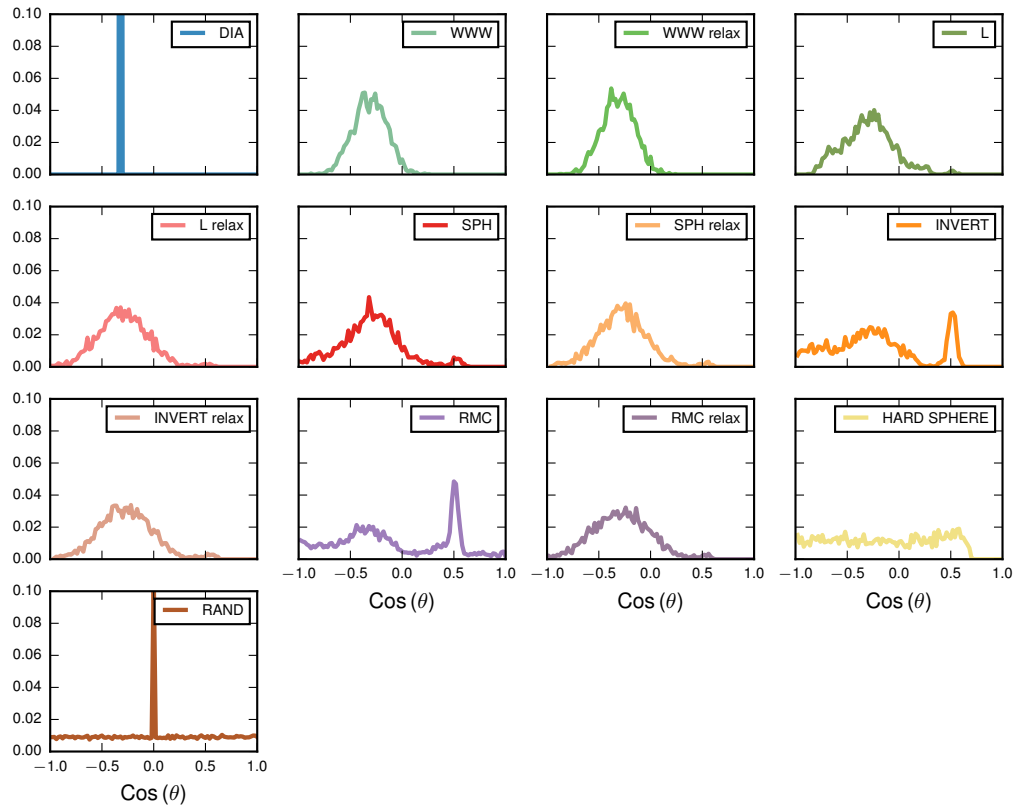
WWW relax The WWW configuration optimised with DFT using the PBE functional until convergence.



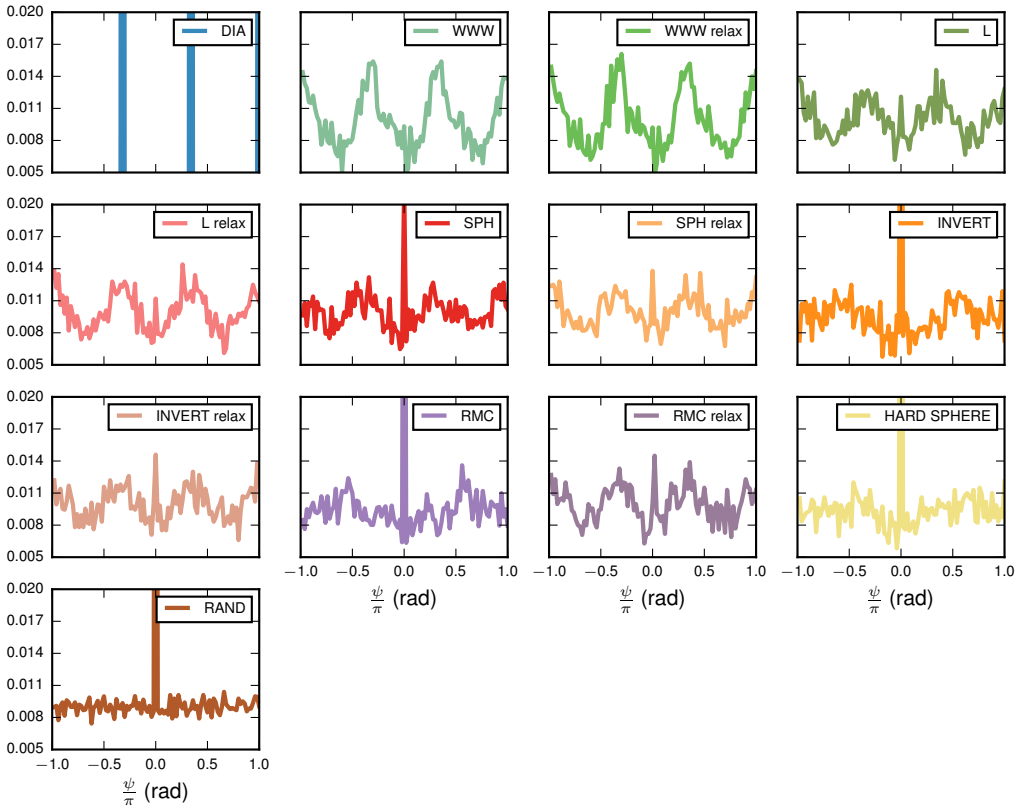
ESI Fig. 1: Histograms of the coordination number distributions for all configurations



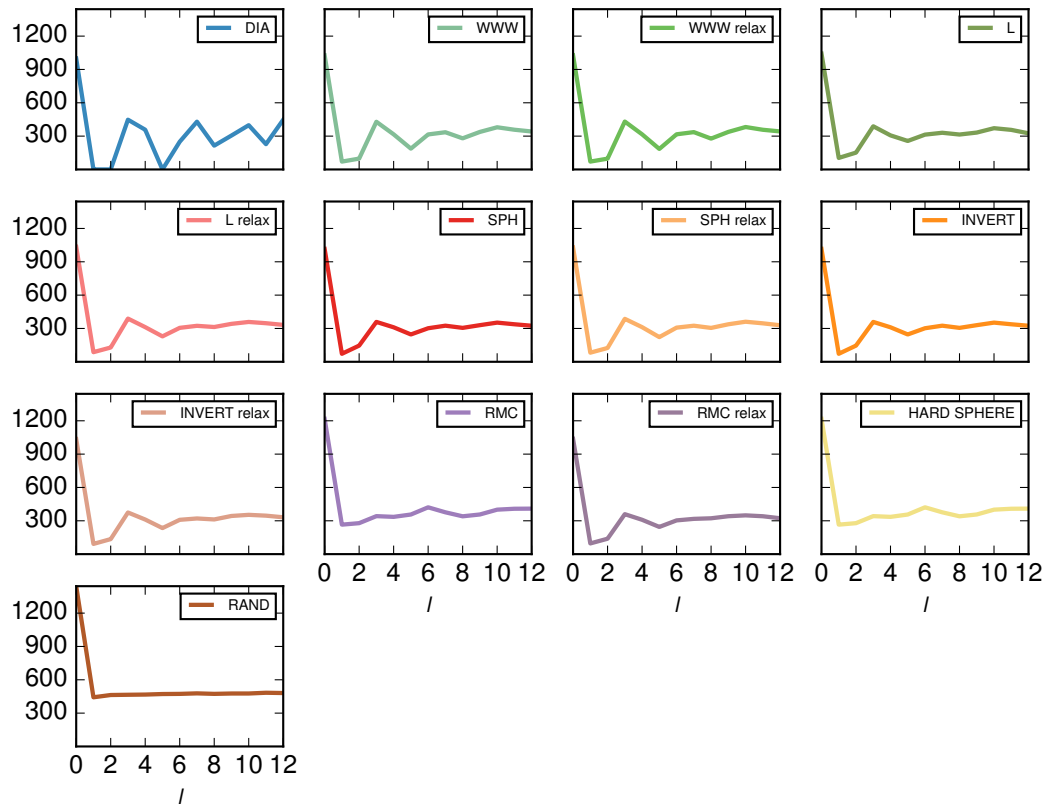
ESI Fig. 2: Pair distribution functions for all configurations



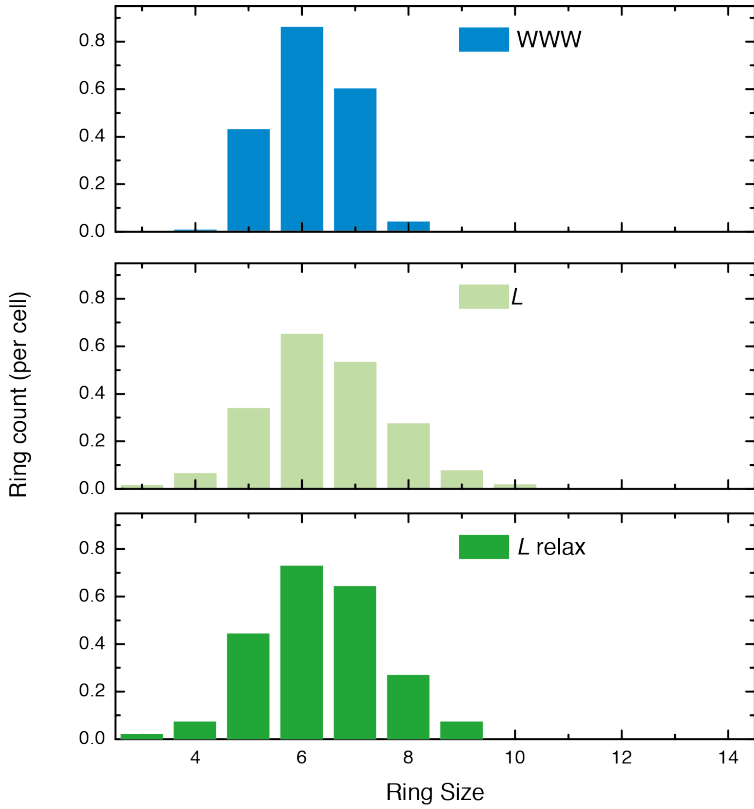
ESI Fig. 3: Histograms of the bond angle distributions for all configurations. The large spike at $\cos(\theta) = 0$ for the random configuration results from near overlapping atoms.



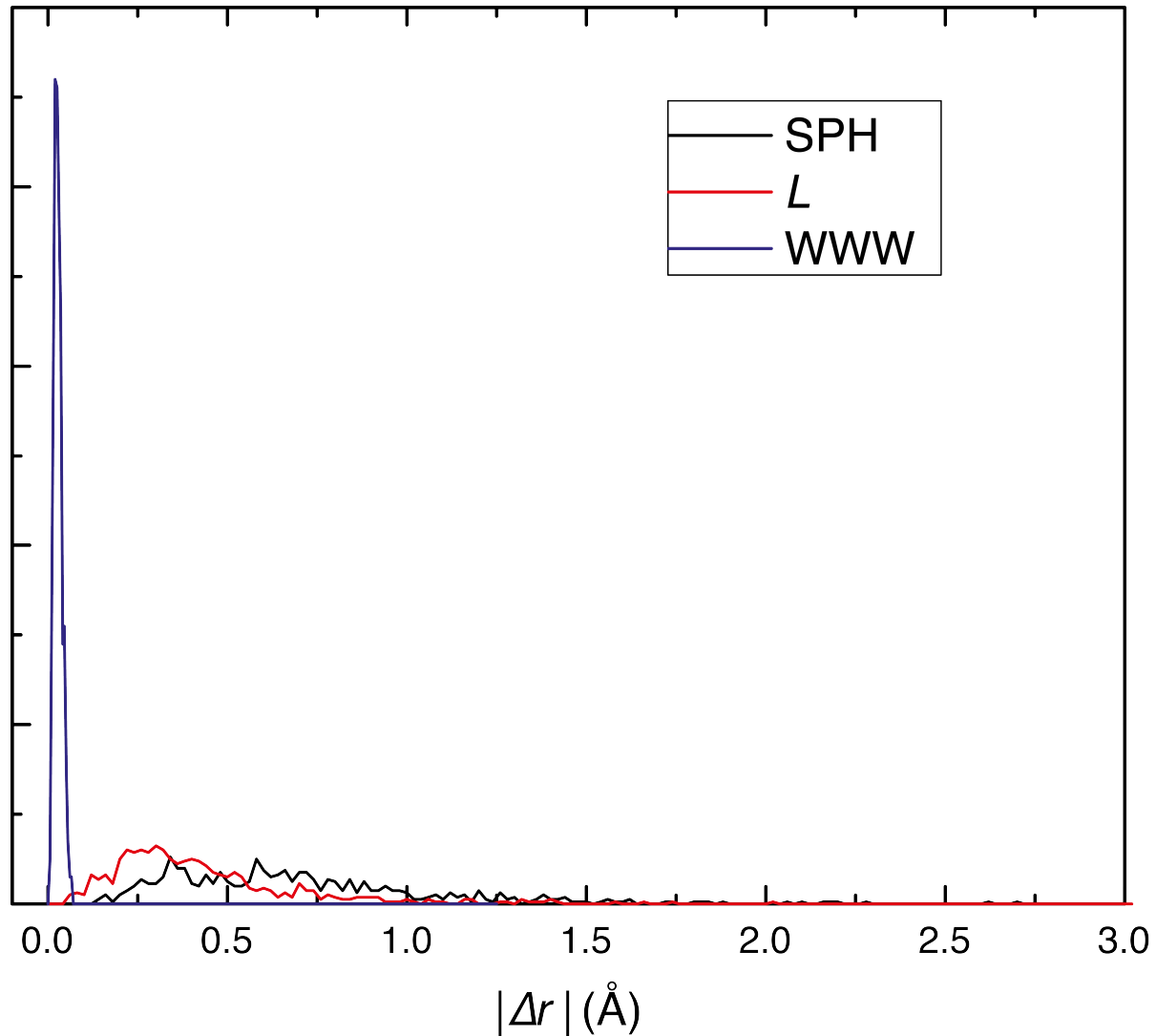
ESI Fig. 4: Histograms of the dihedral angle distributions for all configurations. The spike at $\psi = 0$ results from three-membered rings, which are necessarily completely planar.



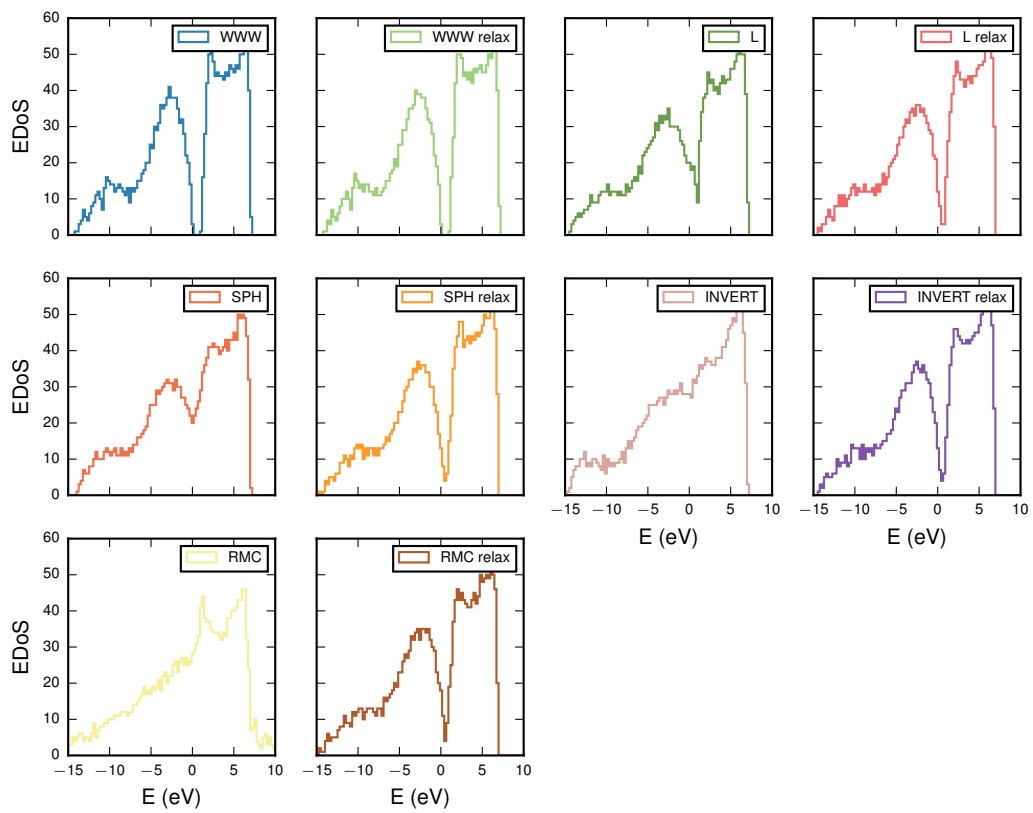
ESI Fig. 5: Calculated average Q_l coefficients for all configurations.



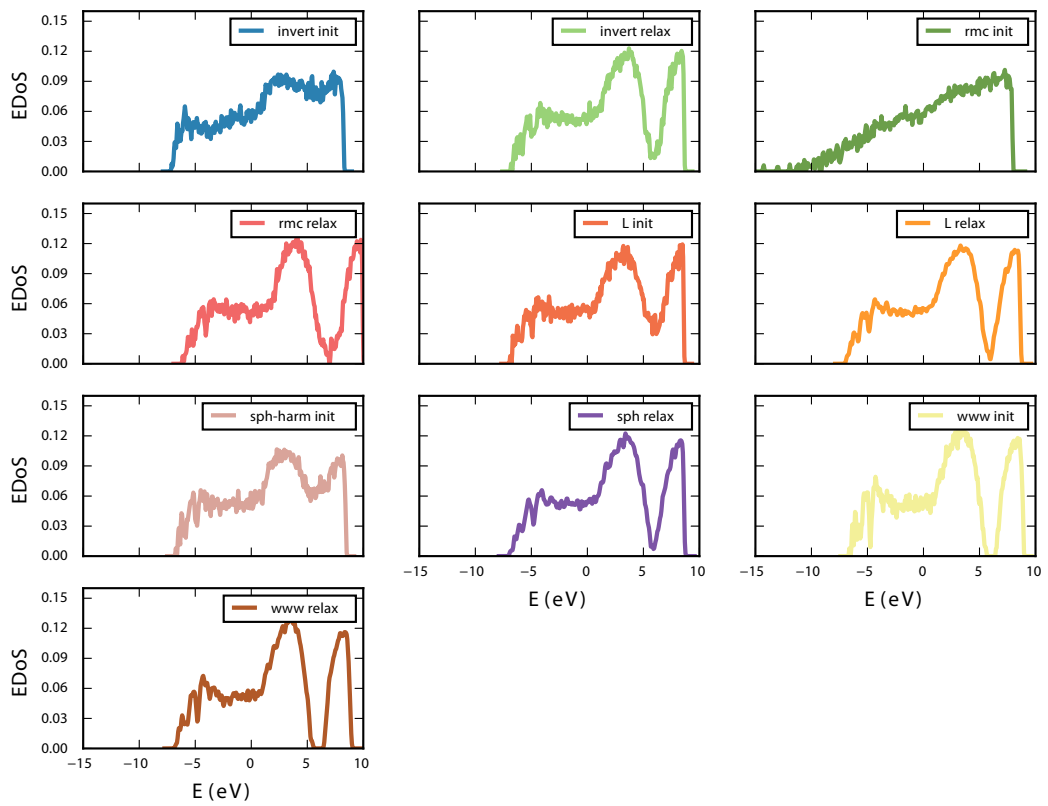
ESI Fig. 6: Ring statistics (using the King's shortest path convention and normalised by number of rings per cell) for the WWW configuration and PDF+*L* refined configuration before and after relaxation. Calculated using ISAACS^{S5}.



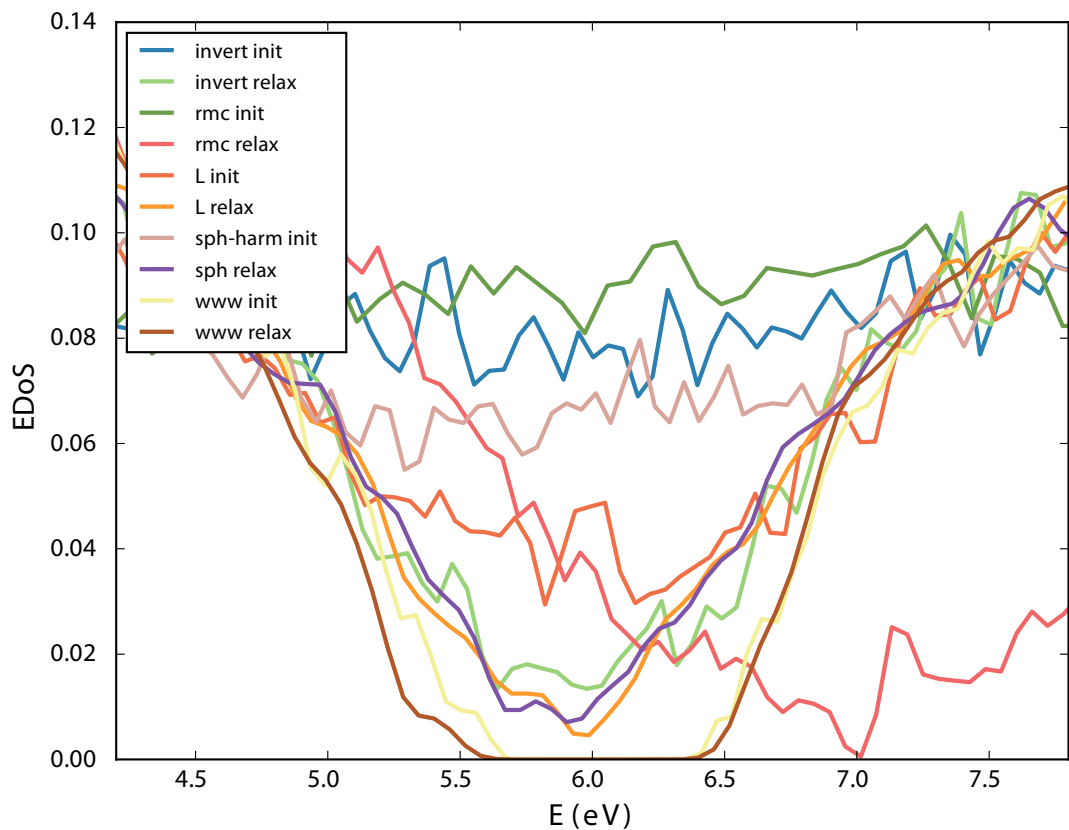
ESI Fig. 7: Histogram of the root square displacement during optimisation for the WWW, SOAP and SPH configurations.



ESI Fig. 8: Electronic density of states calculated using the GSP tight-binding Hamiltonian^{S6}.



ESI Fig. 9: Electronic density of states calculated using DFT and the MBJ functional.



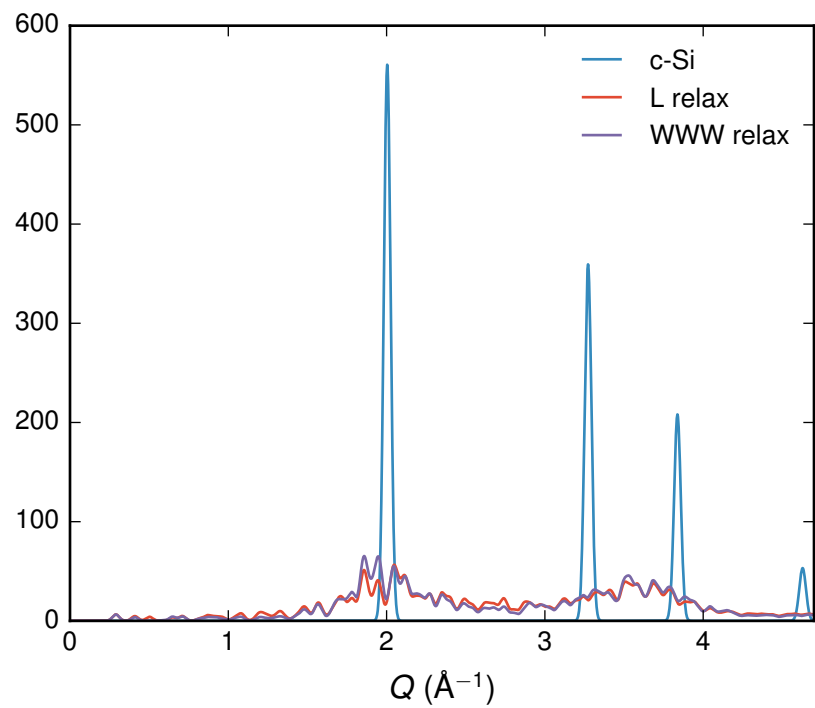
ESI Fig. 10: Electronic density of states calculated using DFT and the MBJ functional, around the gap.

ΔE (eV/atom)	WWW	L	SPH	INVERT	RMC
PBE unoptimised	0.15818068	0.401097615	0.515364201	0.698205189	6.361609732
PBE optimised	0.157081969	0.271789	0.260181578	0.277312328	0.299999896

ESI Table 1: Calculated DFT energies (using the PBE functional) for the optimised and unoptimised configurations of Si, relative to a configuration of crystalline Si.

$\log_{10}(\chi^2)$	WWW	WWW relax	L	L relax	SPH	SPH relax	INVERT	INVERT relax	RMC	RMC relax	hard sphere	random
χ^2_{PDF}	-4.58	-4.77	-6.08	-4.65	-6.18	-4.53	-5.35	-4.46	-5.95	-4.39	-3.89	-3.86
χ^2_{INVERT}	-1.52	-1.52	-1.31	-1.39	-1.28	-1.42	-1.90	-1.37	-0.42	-1.33	-0.95	-0.30
$\text{Var}(Q_l)$	-1.11	-1.10	-1.03	-0.99	-0.99	-0.97	-0.94	-0.97	0.20	-0.91	-0.41	0.35
$1/S$	-0.82	-0.82	-0.63	-0.70	-0.61	-0.73	-0.50	-0.67	-0.40	-0.66	-0.46	-0.18
L	-2.19	-2.16	-1.95	-1.67	-1.82	-1.62	-1.31	-1.60	-0.79	-1.54	-0.90	-0.67

ESI Table 2: Calculated metrics for the full range of configurations (presented as logarithms for ease of comparison.) The metrics are: the fit to the PDF calculated from a 4096 atom configuration generated using the WWW algorithm; the PDF variance measured using the INVERT metric; the variance of the bond orientational order coefficients, Q_l ; the reciprocal of the symmetry measure S and the SOAP similarity measure L . The anomalously high values of χ^2_{PDF} for the WWW and relaxed configurations arise from misfits in the width of the nearest neighbour peak relative to the reference 4096 WWW derived configuration.



ESI Fig. 11: Calculated powder X-ray diffraction patterns created using the CrystalDiffract software of three configurations, illustrating the lack of long-range order for the *L* and WWW configurations.

References

- (S1) M. J. Cliffe, M. T. Dove, D. A. Drabold, A. L. Goodwin, *Phys. Rev. Lett.* **104**, 125501 (2010).
- (S2) M. J. Cliffe, A. L. Goodwin, *Phys. Status Solidi B* **250**, 949 (2013).
- (S3) A. P. Bartók, R. Kondor, G. Csányi, *Phys. Rev. B* **87**, 184115 (2013).
- (S4) G. Barkema, N. Mousseau, *Phys. Rev. B* **62**, 4985 (2000).
- (S5) S. Le Roux, V. Petkov, *J. Appl. Crystallogr.* **43**, 181 (2010).
- (S6) L. Goodwin, A. J. Skinner, D. G. Pettifor, *Europhys. Lett.* **9**, 701 (1989).